geotechnics

Article

Microstructure and Strength Parameters of Cement-Stabilized Loess

Mani Axel *, Xi'an Li, Feng Wen and Ming-Xiao An

Department of Geological Engineering and Geomatics, Chang'an University, Xi'an 710064, China
* Correspondence: maniaxel2012@yahoo.fr

Abstract: In this study, cement was used as a component to provide a stabilizing effect in order to evaluate the hardness and stability of loess soil. To evaluate the strength properties of loess soil reinforced with cement, samples with four distinct cement concentrations (3%, 5%, 7%, and 9%) and three distinct curing durations (7, 14, and 28 days) were generated. During a series of tests, the flexural strength, direct shear strength, indirect tensile strength, and unconfined compressive strength were determined. An appropriate cement dosage was found, in addition to a durability index that could be used to quantify the effect of water absorption investigations on cement-stabilized loess. Both of these discoveries were made simultaneously. Scanning electron microscopy (SEM) and energy dispersive X-ray fluorescence spectrometry (XRF) examinations were carried out so that the fundamental mechanics of the materials could be comprehended. The results show that the cohesion of cement-stabilized loess is much more sensitive to structure than the friction angle of the material. The increase in shear strength after remoulding is due to cohesion. The SEM study showed that the cement interacted with the loess particles to produce a thick cement network that successfully covered the voids and boosted the mixture's strength parameters. The 28-days UCS for the samples containing 7% cement was the greatest, at 3.5 MPa, while the UCS for those containing 9% cement was 4.78 MPa. The highest flexural tensile strength of 1.98 N/mm^2 was determined after 28 days. The tensile strength after 7 days in samples containing 3%, 5%, 7%, and 9% cement reached a maximum force of 0.15 MPa, 0.23 MPa, 0.27 MPa, and 0.37 MPa, respectively, and increased with each passing day. To achieve the desired level of strength, it is necessary to adjust the proportion of cement. In addition, as the curing period progressed, we observed an increase in the resistance and stiffness of the cement-stabilized loess due to the interactions that take place between the structure and the mineral composition. It is believed that this event was caused by naturally occurring cementation. As a consequence of this reaction, the production of new cementitious materials takes place. The cation exchange that causes the hydration and pozzolanic reaction that leads to the creation of aggregates and interparticle flocculation is responsible for their production. These findings suggest that cement may be utilised as a simple and effective method of loess stabilization, ultimately resulting in improved performance of the loess. Therefore, this study revealed that cement may considerably enhance the microstructure and strength parameters of loess. This research provides important information on cement-stabilized loess that has ramifications for geotechnical investigation, construction, research, and testing to achieve a successful project.

Keywords: loess stabilization; cement; mechanical properties; landslide; microstructure

check for updates

Citation: Axel, M.; Li, X.; Wen, F.; An, M.-X. Microstructure and Strength Parameters of Cement-Stabilized Loess. *Geotechnics* **2023**, *3*, 161–178. https://doi.org/10.3390/geotechnics3020010

Academic Editors: Md Rajibul Karim, Md Mizanur Rahman, Khoi Nguyen and Asif Iqbal

Received: 15 February 2023
Revised: 24 March 2023
Accepted: 27 March 2023
Published: 6 April 2023

1. Introduction

Loess is wind-blown sediment that occurs in arid and semi-dry areas where fine sand, silt, and clay accumulate. China has 640,000 km^2 of loess, accounting for 4.4% of its total land area. Most loess comes from the 317,000 km^2 Loess Plateau in the upper and middle Yellow River. According to Dalei Peng et al. [1], the Loess Plateau has around 300 million inhabitants. Loess is utilised in high-filled foundations, subgrades, and embankments because it is inexpensive and plentiful. Loess as a construction material, on the other hand, is lower in tensile and compressive strength and easily bends. Loess structures are brittle, easily damaged, and weatherproof [2,3]. Loess soils, which are recognised for their collapsibility, they are frequently linked to occurrences of landslides and other types of gradual movement phenomena, such as creep events. The deterioration of soils and slopes is often attributed to rapid creep. Landslides, earthquakes, erosion, and flooding, along with environmental and geological issues, were highlighted by Derbyshire et al. [4] as potential dangers for China's loess soils. Loess collapses vary, increasing the danger of landslides and plate edge failures [5]. Clay and bonding material shortages contribute to collapse. Thus, binding loess particles might limit collapsibility and damage. According to Leng et al. [6], the collapsibility of loess is often inconsistent, which may lead to landslides near plateau edged. These calamities are caused by the interparticle brittleness of loess. The vulnerability of loess interparticle interactions continues to be the primary cause of catastrophic tragedies. There are resistance-boosting methods to fix these concerns. Resistance improvement strategies have been presented as a solution to these issues. They include strengthening and stabilizing interparticle interactions [7]. Microstructural research is an efficient method to fully understand the presentation features of loess and to establish the relationships between micro- and macrostructures [8]. According to Ian Jefferson [7], hardening and strengthening interparticle connections to stabilize loess slopes in geotechnical engineering, especially in China, remain challenging. Loess landslides have been studied to ensure engineering safety, leading to the development of effective loess instability prevention and mitigation techniques [9]. Crawford et al. [10] proposed and confirmed a constitutive equation for dynamic hydrological monitoring for landslide detection whereby loess is stabilized to strengthen and endure these obstacles. Lime, cement, and fly ash are among the cementitious materials used worldwide to stabilize soil for better engineering performance.

Much research has been conducted to elucidate the effect of cement on the mechanical behaviour of soil [10]. Researchers found that cement inclusion improves the mechanical properties of soil [11]. Ordinary Portland cement (OPC) is the industry-standard binder for stabilization and solidification because of its effectiveness, cheap cost, availability, and dependability [12]. Liu et al. [13] reported that cement can enhance the microstructure of loess, increase the clay content, and speed up cementation, making the soil stronger. The hydration, pozzolanic reaction, and cation exchange of cement may lead to agglomeration of small soil particles and the formation of chemical bonds. This could improve the geotechnical qualities of problematic soil, including plasticity, strength, stiffness, and durability. Cement stabilization is most effective for low to medium sticky soil and less effective in excessively plastic soil [14]. "Cement is the most common binder used in the deep mixing process. Common cement percentages in Japan and the United States are 20–30% and 10–50%" [15]. Ordinary Portland cement (OPC) is the major stabilizing agent among all hydraulic binders used for stabilization. A reasonable proportion of cement, in addition to boosting saturated strength, improves water erosion resistance both immediately and in the long term. Shenbaga R. [16] and Sathya Subramanian [17] showed that the cement concentration, packing density, moisture content, curing conditions, mineralogy, and physical qualities of the sand all interact in complicated ways, making it difficult to characterise the unconfined compressive strength of cemented soil. According to the previous studies, cement is an excellent soil development method and the best material for stabilizing loess, producing amazing results. If cementing agents' correct loess, the binder concentration increases optimal water content. Insufficient research has been conducted on the interaction between stabilized soil microstructure and strength parameters since engineering tests have often been used to assess the improvement impact.

In light of the aforementioned factors, in this study, we explored the strength parameters of cement-stabilized loess samples with varied cement ratios before performing quantitative analysis SEM and XRF data to identify the pattern of evolution of microstructural parameters inside the pores. The novelty of this research is that it provides a detailed analysis of cement-stabilized loess specimens, their microstructural features, and how the physical and chemical interactions between cement and loess particles create configurational strength.

2. Materials and Methods

2.1. Raw Materials

China's Loess Plateau provided test soils. Four soil samples were assessed for specific gravity (Gs) using an ultra-pycnometer, and the average was considered typical (Table 1). The soil compaction curve showed that 12.00% moisture was optimal and 1.82 g/cm^3 was the maximum dry density. The soil liquid limit (LL) was 31.33% and the plastic limit was 18.33%. (Table 1). The particle size distribution is displayed in (Table 1). Clay, silt, and sand fraction sizes vary. Loess' chemical composition (Table 2) varies based on its location and geological history. Silicon is a prevalent element found in loess, accounting for most of the sediment's mineral composition. Aluminium, iron, magnesium, calcium, and potassium are other frequent components found in loess.

Table 1. Physical properties of loess.

Property	Value
Gs	2.71
ρ_{max} (g/cm^3)	1.82
w_{opt} (%)	12.00
Atterberg limits	
Liquid limit (%)	31.33
Plasticity index (%)	15.00
Plastic limit (%)	18.33
Particle size distribution	
Sand, 0.05–2.0 mm	19.43%
Silt, 0.002–0.05 mm	73.98%
Clay, <0.002 mm	7.59%

Table 2. Chemical compositions of the studied loess.

Chemical Name	SiO_2	$A1_2O_3$	CaO	Fe_2O_3	MgO	K_2O	Na_2O	TiO_2
%	59.47	14.72	11.82	5.07	3.21	2.79	1.59	0.72
USDA classification	Silt loam							
Minerals present	Kaolinite and illite							

Other elements (Table 3), like copper, zinc, and manganese, may be found at trace levels in loess. These trace elements may provide important details about the geological and environmental history of the location where the loess was formed.

Table 3. Elemental composition of loess.

Elemental Analysis	Si	Ca	A1	Fe	K	Mg	Ti
%	52.84	16.38	13.21	8.09	4.87	3.26	1.04

P.O. 42.5 regular Portland cement from Tongchuan Dongguan Cement Co., Ltd., was used in the experiments. (Tables 4 and 5) provide representative chemical compositions and essential features.

Table 4. Chemical compositions of ordinary Portland cement.

SiO_2	Al_2O_3	Fe_2O_3	MnO_2	SO_3	CaO	Ignition Loss
22.60	4.98	2.90	2.32	2.31	61.60	4.48

Table 5. Basic properties of cement.

Density/(g.cm^{-3})	Specific Surface Area/(m^2/kg)	Setting Time/Min		Flexural Strength/MPa		Compressive Strength/MPa	
3.16	363	Initial	Final	3 d	28 d	3 d	28 d
		170	210	6.3	9.2	26.8	49.7

2.2. Specimen Preparation

The mix ratios were compared to the cement, loess, and water masses. Dry cement and loess were thoroughly mixed. The water-to-loess ratio was 0.4. The original combinations all contained loess and varied in cement content (3%, 5%, 7%, and 9%). After adding water, they were mixed. We kept the mixtures in airtight plastic bags for 24 h to balance the moisture before compaction. The material was crushed in layers within a cylindrical steel mould with a 61.8 mm diameter and a 125 mm height to create a homogeneous cement-stabilized loess. GB/T50123 required 4 layers with 20 knocks each. The samples were 80mm long and 39.1mm wide. Compacted specimens were removed from the mould. They were labelled and sealed. Samples were made and cured for 7, 14, and 28 days.

2.3. Testing Methods

2.3.1. Flexural Strength Test

Steel moulds with dimensions of 105 × 99.5 × 213 mm formed beams for the study (Figure 1a). Next, the flexural tensile strength of the beams was measured, and three homogenous cement–loess layers were moulded. After modification, the moulds were sealed in plastic (Figure 1b) and left overnight. At this point, the samples could sustain their own weight. Demoulded samples were aged for 28 days at 20 °C, with 1 °C relative humidity and temperature. We measured the flexural tensile strength of the beams made from cement-stabilized loess in accordance with PN-EN 12390-5, the European standard for evaluating hardened concrete. According to [18], the flexural strengths of the test specimens were determined. Four different cement samples were used in the study. The samples were built around two 20 mm diameter steel shafts with a 30 cm base. Each beam's load shaft was placed in the centre of its length.

(a) (b)

Figure 1. (**a**) Steel mould (**b**) sample wrapped with plastic.

The following formula was used to compute the flexural tensile strength of each sample:

$$f_t = \frac{3.F.l}{2.d_1 d_2^2} \tag{1}$$

where: d_1 = depth, d_2 = width.

2.3.2. Unconfined Compression Test

Mechanical properties of stabilized soils are often evaluated by measuring their unconfined compressive strength (Figure 2). The unconfined compressive strength test is used in soil stabilization applications to measure loess improvement after treatment. We examined the effect of Portland cement on loess by adding different percentages of cement by weight. Each cylindrical UCS test item was 39.9 mm wide and 80 mm high. The soil–cement samples were placed in a humid and temperature-controlled curing chamber. To characterise the mechanical characteristics of the loess specimens, we estimated their unconfined compressive strength (UCS) using the formula proposed in [19]. Direct compression was applied to the samples, and the displacement rate was measured at 0.01 mm/s.

Figure 2. Unconfined compressive test.

2.3.3. Compaction Test

Compaction tests indicate the appropriate moisture level per Chinese National Standard GB/T50123-2019. Three layers of loess samples with varied water contents filled the squeezed cylinder. Each layer of loess was pounded 25 times. Before compressing the samples, the cylinders were filled. The sample weight was divided by the compressed cylinder capacity to obtain the wet density. The following formula yields the dry density:

$$\rho_d = \frac{\rho_o}{1 + 0.01\omega} \tag{2}$$

The above approach correlates wet and dry densities for each category. The graphs show that the ordinate of the peak point ordinate has the highest water content, and the abscissa has the highest dry density.

2.3.4. Indirect Tensile Strength

The British Standards Institution's indirect tension test method was used to determine the indirect tensile strength of cement-stabilized loess specimens [20].

This test method determines hydraulically bound mixture indirect tensile strength (Figure 3). The specimens analysed had a slenderness ratio of 2.05. Two plywood pieces with dimensions of 4 × 4 × 80 mm were used as bearing strips. Compressed samples were analysed at 0.002 mm/s. A vertical force to two parallel sides of a horizontal cylinder was applied to measure the material's tensile strength, followed by a vertical sample split. This mathematical equation indirectly calculates tensile strength [20]. Indirect tension testing was utilised to evaluate the tensile strength of the stabilized loess specimens. "Test Method for Determining the Indirect Tensile Strength of Hydraulically Bound Mixtures".

Figure 3. Indirect tensile test.

The slenderness ratio was 2.05 (low). The bearing strips were two 4 × 4 × 80 mm wooden pieces. Samples were compressed at 0.002 mm/s. This test measured the tensile strength of a horizontal cylinder using a vertical force on two parallel sides. The sample was sliced vertically into equal parts. The following formula was used to determine indirect tensile strength.

$$R = \frac{2F}{\pi H D} \tag{3}$$

where R is the indirect tensile strength, F is the maximum applied force, H is the length of the sample, and D is the diameter of the sample.

2.3.5. Direct Shear Test

The direct shear test follows the [21] standard (1994). In this study, the shear ring in the cement-stabilized loess was 60 mm × 60 mm × 25 mm. The specimens were then removed from the shear box. The shear strength was measured at 50, 100, 200, and 300 kPa, with a horizontal displacement rate of 0.05 mm/min. Each mixture combination included three specimens, and the test data average was determined. Based on addition proportions (3%, 5%, 7%, and 9%), the samples were divided into 4 groups to assess cohesiveness (c) and internal friction angle (ϕ). Curing took 7 days.

2.3.6. Water Absorption Test

The water absorption and softening coefficient were studied to assess the water resistance of cement-stabilized loess. For the water absorption test, the specimens' dry weight was determined after 28 days, followed by their weight after 1 day in water. The following approaches yielded water absorption:

$$R_n = \frac{M_n - M_0}{M_0} \times 100\% \tag{4}$$

where M_n is the dry mass, and M_n is the water-immersed material. The compressive strength of specimens after 28 days and after 1 day in water were assessed to establish the softening coefficient. The following equation was used to calculate the softening coefficient:

$$K = \frac{l_1}{l_0} \tag{5}$$

where K is the softening coefficient, l_0 is the compressive strength after 28 days, and l_1 is the corresponding compressive strength after immersion in water.

2.3.7. Microstructural Analysis

Many investigations have shown that cementitious components influence the microstructure of compacted mixtures. After 28 days of curing with cement percentages of 3%, 5%, 7%, and 9%, SEM (Figure 4a) was employed. X-ray power diffraction (XRF) showed the usual quartz and clay composition of the loess.

(a) (b)

Figure 4. (**a**) M4 Tornado micro-XRF spectrometer and (**b**) scanning electron microscope.

An XRF spectrometer (Figure 4b) was used to perform non-destructive chemical tests on rocks, minerals, sediments, and fluids. The behaviour of atoms in the X-rays allowed for XRF analysis of primary and trace elements in geological rocks.

3. Results and Discussion

3.1. Compaction Properties

The standard test approach for laboratory soil compaction characteristics was used to perform compaction tests with normal effort. Trace cement in loess soil affected its usual Proctor compaction curves (Figure 5). The maximum dry unit weight decreased from 1.82 g/cm^3 to 1.48 g/cm^3 when the cement concentration was increased from 0% to 9% and the appropriate moisture level increased from 0.12% to 0.14%. The dry unit weight decreased steadily with cement concentration.

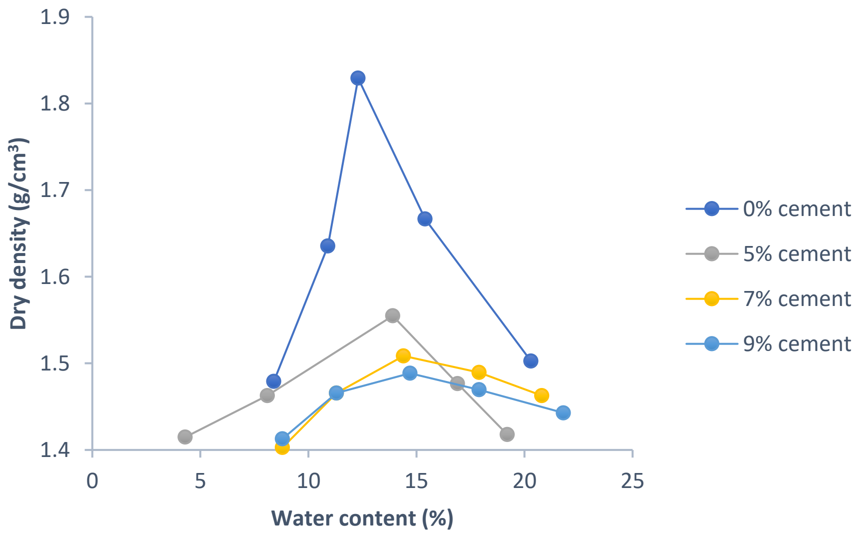

Figure 5. Moisture content–dry density relation curves of cement-stabilized loess.

It was shown that the ideal moisture content increased as a function of cement percentage because cement hydration necessitated an increasing amount of moisture [22]. "These changes may be related to the pozzolanic reaction, as occurs with related clay materials" [23]. The optimal water content increases together with the percentage of binder used to enhance loess [24].

The addition of cement increases flexibility, in agreement with the idea that the optimum water content should increase by around 10%. The inclusion of cement, which has a higher density relative to loess and soil skeletal stiffness, may explain the increased maximum dry density in loess cement mixtures. Cement-stabilized loess develops its final macrostructure as a result of primary cement linkages between aggregated loess and cement particles.

3.2. Shear Strength

The direct shear test was used to measure the shear strength parameter. After 7 days, cement-stabilized loess had a maximum shear strength (Figure 6a). In general, the microstructural modifications that take place in cement-stabilized loess after shear strength testing are complex and depend on a variety of characteristics, including soil composition, the kind and amount of cement used, and the testing circumstances. Shear strength increased steadily as cement content increased. These findings show how cement boosts peak shear strength. As illustrated, cement-stabilized loess strength envelopes determined their friction angle and cohesiveness (Figure 6b,c). The association between cement and friction angle dropped, demonstrating that soil structure had no effect at a certain cement concentration. The friction angle decreased from 27° to 20° as the cement percentage increased from 3% to 7%. The cement percentage increased with shear strength. The 7% cement composite was four times stiffer than the 3% composite. These data reveal that cohesion, which increases shear strength, is more structure-sensitive than friction angle. Remoulded samples with cement percentages under 9% demonstrated minimal friction angles. Cementitious linkages between loess mineral components create a matrix that encloses unbonded particles and aggregates, resulting in more complex engineering behaviours [25].

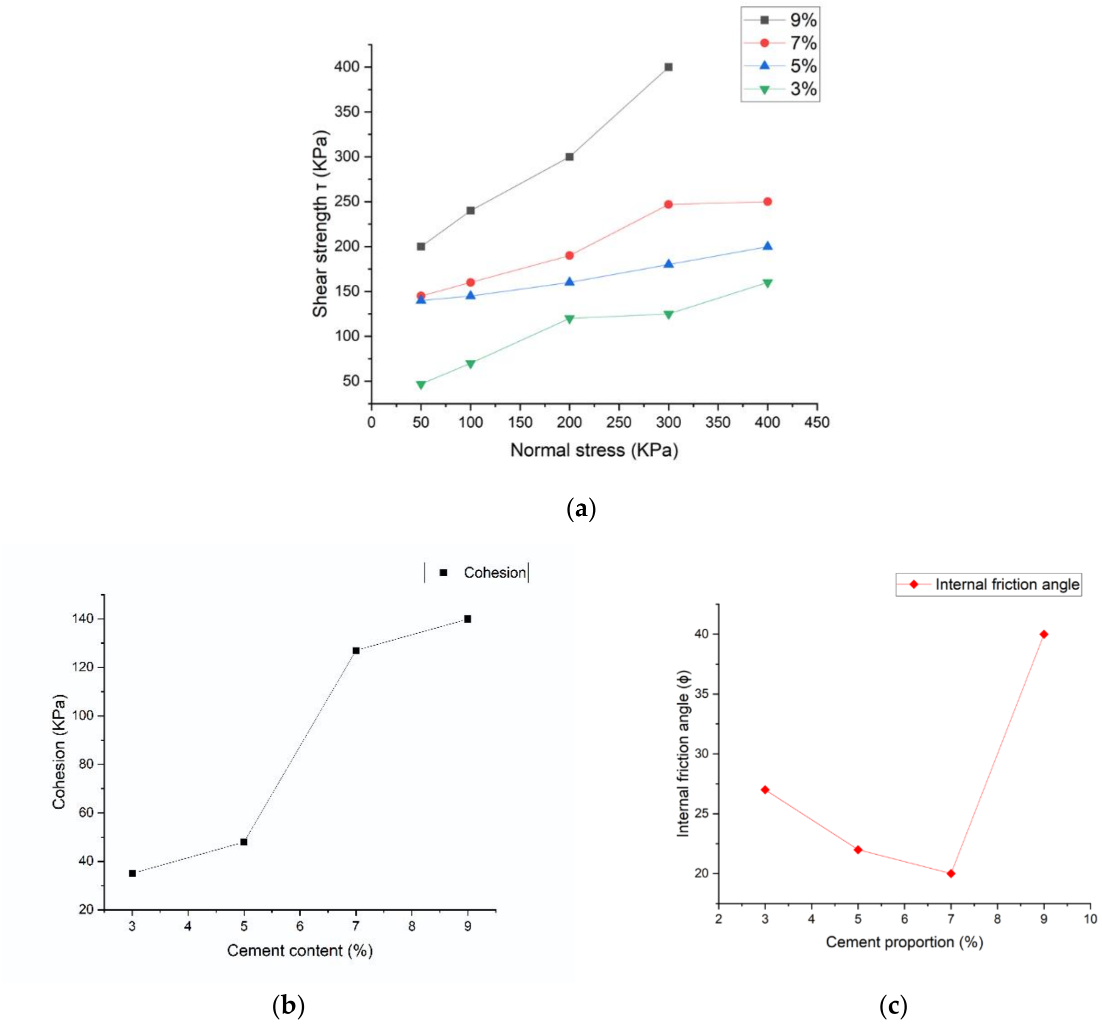

Figure 6. The relationships between shear strength parameters and cement proportion of cement-stabilized loess: (**a**) representative peak shear strength (τ) envelopes; (**b**) cohesion (c) relative to cement proportion; (**c**) internal friction angle (ϕ) relative to cement proportion.

3.3. Unconfined Compressive Test

The unconfined compressive strength (UCS) test is a typical technique for determining the strength of cement-stabilized soils. In this case, the loess was stabilized with different percentages of cement (3%, 5%, 7%, and 9%) and cured for varying lengths of time (3 days, 14 days, and 28 days). The UCS tests demonstrate that increasing the cement quantity and curing time enhanced the strength of the stabilized loess. Consoli et al. [26] discovered that the unconfined compressive strength of cement-stabilized soil improves proportionally as cement content increases. The UCS of cement stabilized-loess (Figure 7) after 7 days varied from 0.75 MPa for 3% cement to 1.4 MPa for 9% cement. The UCS increased dramatically after 14 days, with values ranging from 1.25 MPa for 3% cement to 2.75 MPa for 9% cement. The UCS continued to increase after 28 days, with values ranging from 1.4 MPa for 3% cement to 4.78 MPa for 9% cement.

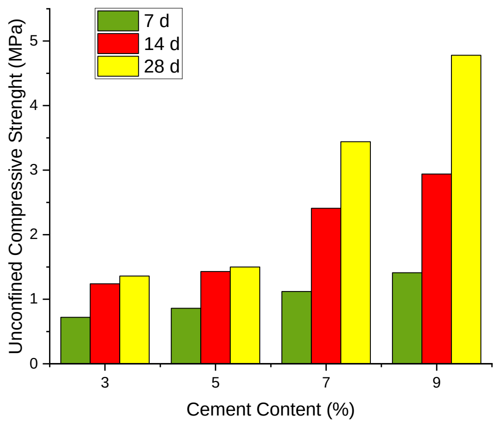

Figure 7. Variation of unconfined compressive strength relative to cement content.

The development of cementitious compounds in the microstructure of the stabilized loess was responsible for the increase in strength. When cement is mixed with loess, it interacts with water to generate cementitious compounds such as calcium silicate hydrates and calcium aluminate hydrates, which fill the pores and bind the soil particles together. These chemicals continue to develop and enhance the microstructure of the stabilized loess as the curing period advances. Moreover, the increased degree of compaction and decrease in the void ratio owing to the cement stabilization process might contribute to strength enhancement. The cement stabilizes soil particles by creating chemical links with the minerals in the soil, lowering the soil's sensitivity to moisture fluctuations and boosting its overall strength and durability.

Finally, the UCS test findings show that cement stabilization is a viable strategy to increase the strength of loess soils. The increased strength is attributable to the production of cementitious compounds in the microstructure of the stabilized loess, as well as an increase in compaction and a decrease in void ratio. The reported test findings may help engineers and construction professionals to plan and choose suitable stabilization techniques for loess soils in a variety of engineering applications.

3.4. Flexural Strength

The flexural strength of cement-stabilized loess is a measure of the material ability to resist bending or deformation under a load. The flexural strength parameters of cement-stabilized soils were examined in [27]. Flexural strength is a crucial characteristic for the fatigue analysis of cement-stabilized loess. (Figure 8) shows the flexural strength of the cement-stabilized loess measured after 28 days for four different percentages of cement used in the stabilization process: 3%, 5%, 7%, and 9%. The results show an exponential increase in flexural strength as the percentage of cement increases. Cement strengthened the structure, as planned. Cement improved strength by 0.8 N/mm^2, 1.1 N/mm^2, 1.4 N/mm^2, and 1.98 N/mm^2 for 3%, 5%, 7%, and 9%, respectively. An exponential increase in flexural strength means that the strength increases at an accelerating rate with increasing percentages of cement. Several microstructural changes happen when the flexural strength of cement-stabilized loess is tested. When water is added to cement-stabilized loess, it starts a chemical reaction called cement hydration. This process results in a complex network of crystals that fit together. This can make the material stronger and last longer. Secondly, as the loess is subjected to stress during the flexural strength test, the particles can rearrange themselves, causing a change in the microstructure of the material. This can lead to an increase in density and a reduction in pore space, which can improve the strength of the material. Ettringite and C-S-H gel provide strength, and humidity optimises hydration. Cementing loess modifies its failure mechanisms. Cement-stabilized loess samples maintained strength throughout the test.

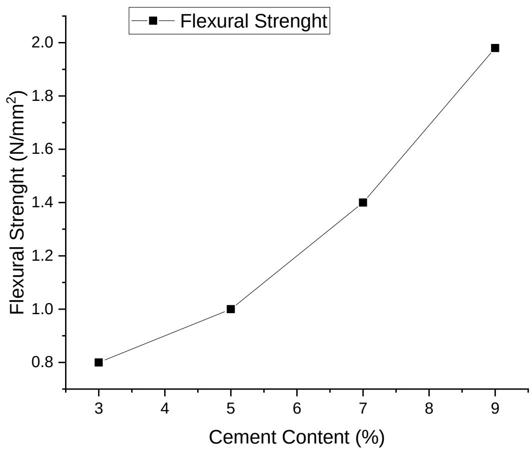

Figure 8. Flexural strength of cement-stabilized loess after 28 days of curing.

3.5. Splitting Tensile Strength Test

According to the research conducted by Consoli et al. [28], the strength of stabilized soil improves as the volumetric binder concentration increases and declines as the porosity increased. The splitting tensile strength of cement-stabilized loess is defined as the amount of tensile stress that the loess can handle without cracking. The results show that the strength of cement-stabilized loess increased with the amount of cement and the curing time.

The splitting tensile strength (Figure 9) of 3% cement added after 7 days was 0.15 MPa, increasing to 0.23 MPa after 14 days and 0.37 MPa after 28 days. This increase in strength is attributable to the hydration of the cement, which leads to the development of hydrated compounds such as calcium silicate hydrate (C-S-H) gel, which is responsible for the increase in strength in the cement-stabilized loess.

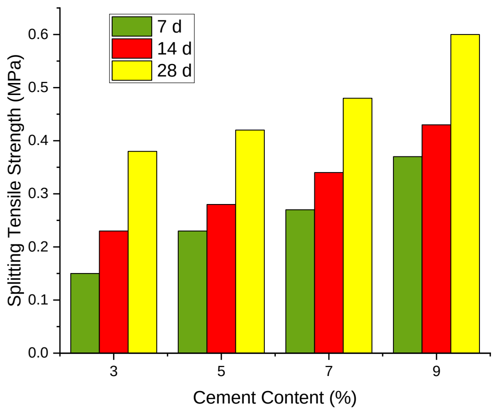

Figure 9. Variation of tensile strength relative to cement content.

Furthermore, the addition of 5%, 7%, and 9% cement led to an increase in splitting tensile strength with increasing curing time. After 28 days, the splitting tensile strength was 0.42 MPa for 5%, 0.48 MPa for 7%, and 0.57 MPa for 9% cement content. Notably, the appropriate cement concentration to obtain the necessary splitting tensile strength relies on a number of variables, including the features of the loess and the planned use of the stabilized material. The reported results show that higher cement concentrations usually lead to higher strength, although this is not always the case. High cement content may contribute to the production of shrinkage fractures caused by the excessive heat created during hydration, resulting in a reduction in splitting tensile strength. The microstructure of cement-stabilized loess is critical to the development of splitting tensile strength. The addition of cement enhances the concentration of C-S-H gel, which fills the pores and gaps of the loess to produce a more compact and dense microstructure. Increased splitting tensile strength is a result of a denser microstructure. Furthermore, the splitting tensile strength of cement-stabilized loess can be affected by the way in which it is compacted, how it is allowed to cure, and the presence of other materials, such as pozzolanic materials.

Understanding the splitting tensile strength and microstructural changes that occur throughout the stabilization process is crucial for developing and choosing cement compositions to stabilize loess materials that satisfy the requisite strength parameters.

3.6. Flexural–Compressive Strength Relationship

Flexural and indirect tensile strength are as important as unconfined compressive strength for assessment of material stabilization. Figure 10 shows flexural and unconfined compressive strengths at different cement concentrations (with an R value of 0.71). The material was homogeneous, since the UCS and flexural strength samples were different. The findings can be compared and connected, but they are not reliable.

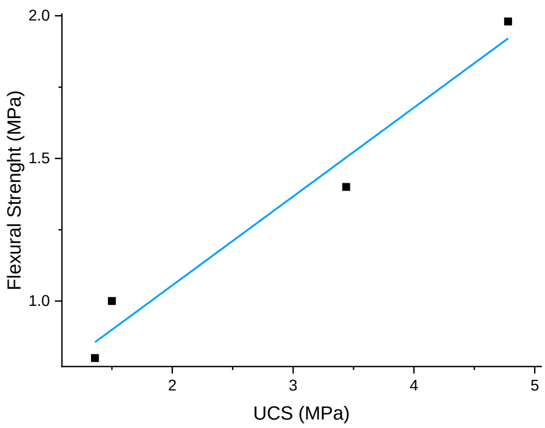

Figure 10. Comparison of relationships between UCS and FS.

3.7. Water Resistance

Using different samples of cement and loess, the effect of curing time on how much water a material can hold was studied. The soaking process increased R_n from 30 min to 24 h, as seen in (Figure 11). The water absorption rate quantifies a material's capacity to resist water penetration. According to the result, the rate of water absorption decreases as the amount of cement increases. The water absorption rate was greatest with 9% cement content, at 2.7% for 30 min, 2.6% for 60 min, 2.6% for 90 min, and 3.5% for 24 h. The water absorption rate was 0.5% for 30 min, 1.1% for 60 min, 1% for 90 min, and 1.3% for 24 h for 3% cement. The microstructure of cement-stabilized loess is crucial in influencing the material's water resistance. The inclusion of cement in loess raises the material's density and provides a binding matrix that decreases the porosity. This causes a drop in the material's water absorption rate. With increasing cement content, the microstructure becomes denser and less porous, resulting in decreased water absorption rates. Calcium silicate hydrate (C-S-H) and calcium hydroxide ($Ca(OH)_2$) must form, as cement hydrates during the curing process of cement-stabilized loess. The C-S-H gel fills the spaces between the particles and makes the material denser. $Ca(OH)_2$ is forms as a by-product, which plugs the pores. The C-S-H gel continues to develop as the curing period continues, resulting in a denser microstructure with fewer holes. This leads to an increase in the material's water resistance.

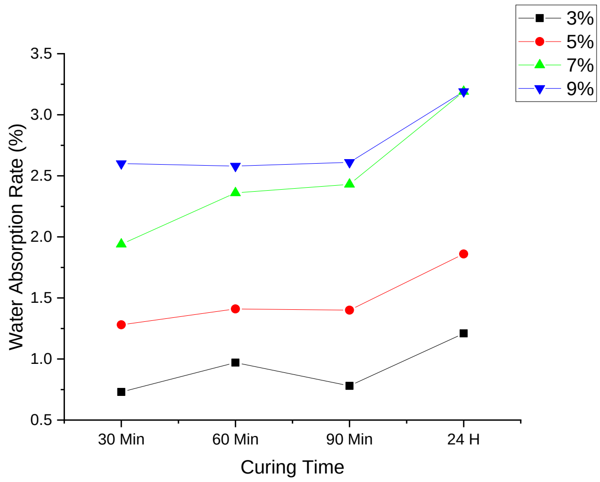

Figure 11. Influence of soaking time on water absorption rate.

The curing duration also significantly impacts the water resistance of cement-stabilized loess. After 24 h of curing, the water absorption rate rose dramatically for all cement percentages. This might be because the material was not completely cured and still had a large porosity, allowing it to absorb more water.

The ability of cement-stabilized loess to resist water can be improved by adding more cement and giving it more time to cure. A material's microstructure largely determines how resistant it is to water, with a denser and less porous microstructure resulting in lower water absorption rates.

3.8. Microstructure Analysis

3.8.1. XRF Analyses

Cement-stabilized loess was analysed by XRF. Micro-XRF (M4 Tornado, German) was used to measure the elemental composition (Table 6, Figure 12). XRF (X-ray fluorescence) analysis is a non-destructive method for determining a material's elemental composition. XRF analysis can provide information regarding the distribution of elements in the microstructure of cement-stabilized loess.

Table 6. Physical, mineralogical, and elemental composition of the soil.

Compound	Concentration (%)	Chemical Composition	Content (%)
Al	1.72	Al_2SO_3	3.25
O	18.58		
Si	6.95	SiO_2	14.86
P	0.00	P_2O_5	0.00
S	0.09	SO_3	0.23
Cl	49.90		
K	2.31	K_2O	2.79
Ca	12.09	CaO	16.92
Ti	0.61	TiO_2	1.01
V	0.03		
Mn	0.15	MnO	0.20
Fe	7.54	Fe_2SO_3	10.79
Zn	0.03	ZnO	0.00
Rh	0.00		

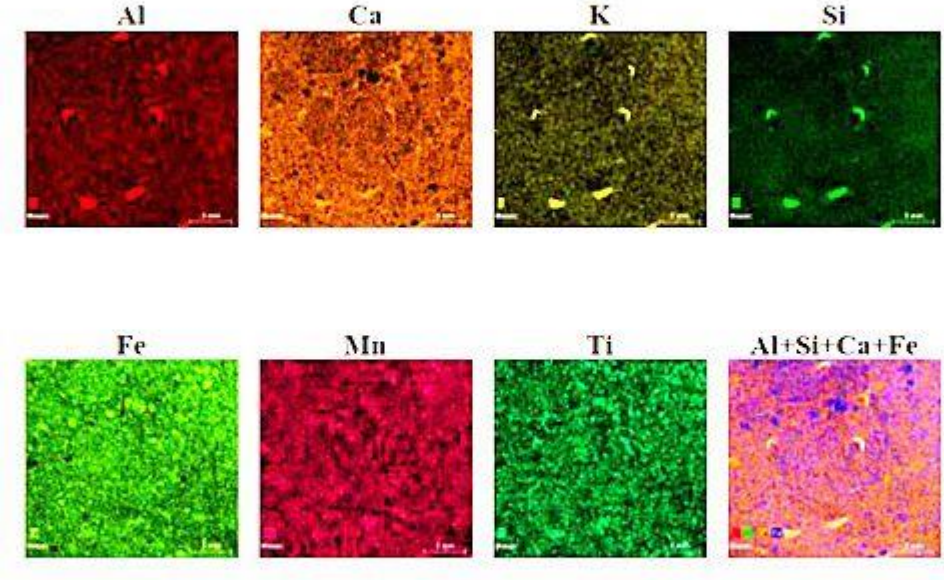

Figure 12. Elemental images of a silt loam captured using micro-XRF.

XRF analysis shows (Table 6) that the sample of cement-stabilized loess has the most of the elements Si, Ca, and Al. Si makes up 6.95% of the sample, which shows that the loess contains silica (SiO_2). Calcium makes up 12.09% of the total, which shows that calcium carbonate ($CaCO_3$) is present, which is a common mineral in loess. Al amounts to 1.72%, showing that aluminum silicates are present in the loess.

Along with the main elements, there are also smaller amounts of Fe, K, Mn, and Ti. Fe accounts for 7.54% of the total, showing that iron oxide (Fe_2O_3) is present in the loess. 2.31 percent K indicates the presence of potassium oxide (K_2O). Mn and Ti are considerably less abundant, accounting for 0.15% and 0.61% of the sample, respectively.

The XRF analysis also provides information regarding the loess' mineral composition. The SiO_2 content of 14.86% indicates the presence of quartz, a common mineral found in loess. The Al_2O_3 concentration of 3.25% indicates the existence of aluminum silicates, such as feldspar or mica. A CaO concentration of 16.92% shows calcium carbonate is present. The Fe_2O_3 content of 10.79% suggests the presence of iron oxide. The K_2O content of 0.37% suggests the presence of potassium feldspar. According to [29], the maximum SO_3 concentration is 4%.

Adding cement to the loess microstructure can result in a number of alterations. For instance, cement may serve as a binder, therefore increasing the material's strength. Additionally, cement can fill the spaces between soil particles, resulting in a decrease in porosity and permeability. This may increase the material's water resistance and longevity, which is especially important in construction situations where the material may be exposed to damp.

The XRF analysis of cement-stabilized loess tells us a lot about the elements and minerals that make up the material. This information can be used to learn about the microstructure of the material and how stabilization with cement changes the properties of loess. The XRF analysis can also be used to improve the design of cement stabilization processes and make sure that the final product is of high quality.

3.8.2. SEM Analyses

The SEM micrographs (Figure 13) show the microstructure of cement-stabilized loess after 28 days with 3%, 5%, 7%, and 9% cement percentages. The dominant crystalline hydrates in the examined patterns were $Ca(OH)_2$ and ettringite [30,31] Reaction products and hydration affect loess matrix changes (Figure 13a). According to Angelova and Evstatiev [32], the particles and pores of the soil are partially covered and filled by fibrous phases of about 0.5–1.0 m in length. Fibrous growths can be seen in the sample because the loess matrix is porous and the composite mixture has a high water-to-cement ratio. At higher magnification, hydration product production was fast (Figure 13c). As cement concentration increases, natural soil flocculations thicken. Cement-produced flocculations may create a stronger, more controllable loess structure with denser particles. Thus, increasing the cement dose improved flocculation and loess strength. This result may be explained by recognising that the flocculations are a consequence of the cement hydrating during the curing time and that additional cement would result in increased hydration, cementing weak soil particles and enhancing soil strength. C-S-H gel hydration products form the reticular fibrous network after 28 days (Figure 13d). Calcium silicate hydrate (C-S-H) is thought to boost Portland cement's strength when hydrated. Soil stabilized by $Ca(OH)_2$ from cement hydration may be further strengthened via C-S-H synthesis, which involves the ionisation of Ca^{2+} and OH^-. Calcium and alumina may produce a C-A-H cementitious complex. Ettringite grew with C-S-H phases ($3CaO.Al_2O_3.3CaSO_4.32H_2O$ or C6AS3H323CaO).

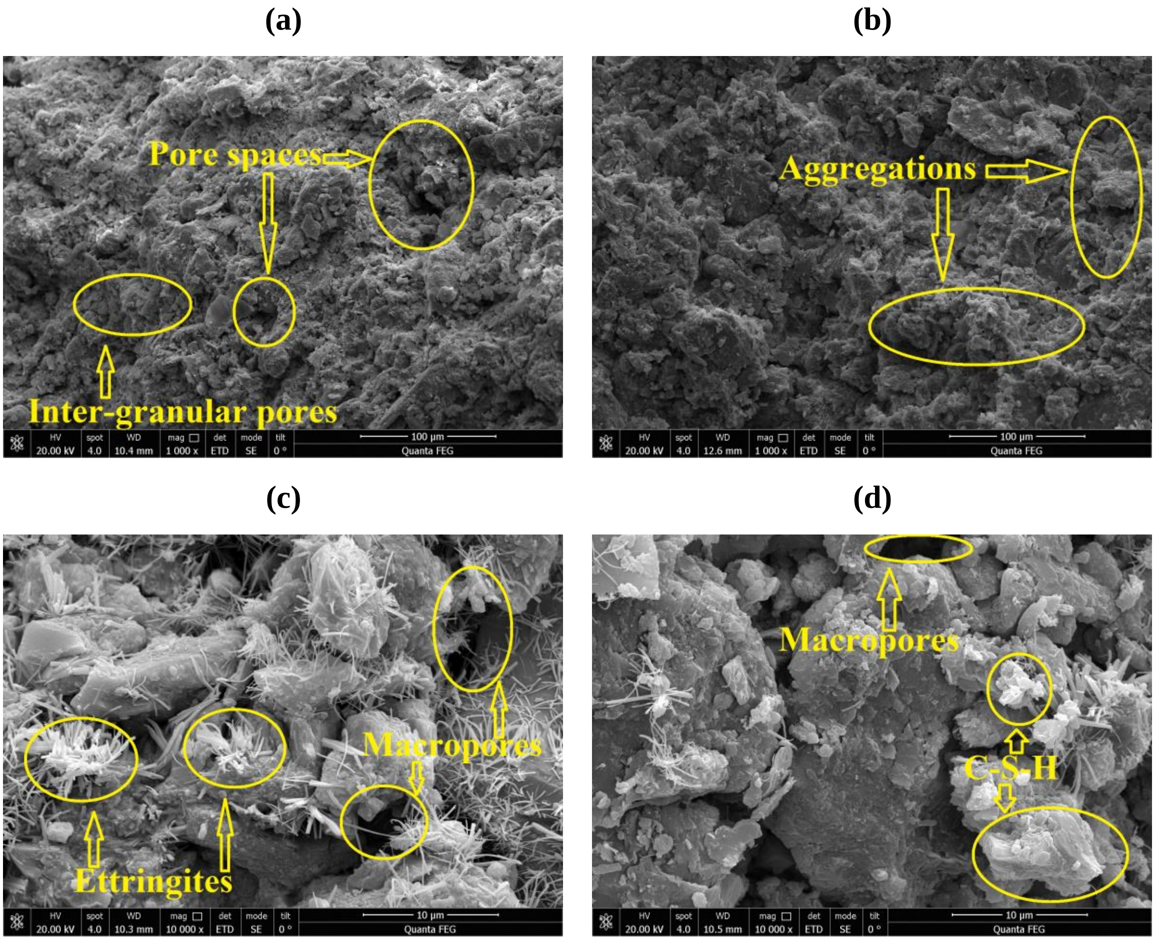

Figure 13. SEM photomicrograph of loess stabilized with (**a**) 3% cement, (**b**) 5% cement, (**c**) 7% cement, and (**d**) 9% cement.

The cement-stabilized loess's strength is provided by additional cementation products created during curing. Cation exchange, pozzolanic reactions, and carbonation strengthen cement-stabilized loess. Cement-stabilized loess aggregates during short-term cation exchange, increasing its strength. Slow pozzolanic reactions and carbonation create new cementitious materials, make loess particles less porous, and bond soil particles. This makes cement-stabilized loess considerably stronger.

$$Ca(OH)_2 + SiO_2 \longrightarrow C\text{-}S\text{-}H$$

$$Ca(OH)_2 + Al_2O_3 \longrightarrow C\text{-}A\text{-}H$$

4. Conclusions

Loess from the "China Loess Plateau" was tested for geotechnical properties after being combined with different cements. The water resistance, density, and compressibility of cement-stabilized loess were measured. The direct shear, as well as the flexural, unconfined compressive, and tensile strengths, was also measured to compare strength at various curing stages. Results:

(1) Cement minimises loess flexibility. Increasing shear strength correlated with changes in cohesiveness. This study shows that cohesiveness in cement-stabilized loess is more structure-sensitive than friction angle and that bonding is necessary for shear strength gain following remoulding.
(2) The compressive strength increases without limit as the cement amount and curing time increase. The unconfined compressive strength of a given cement content increases as curing time increases.
(3) With more cement added and the ideal moisture level decreased, the maximum dry density increases.
(4) Tensile and bending strengths grow with the quantity of cement used and the curing period.
(5) After 28 days, the specimens' flexural strength increased most when the cement concentration was between 7% and 9%.
(6) Cement pozzolanic reaction enhanced the strength properties of the loess by creating ettringite and C-S-H gels.

The findings of this study require addition research into strength factors. Importantly, testing the long-term effectiveness of loess cement stabilization under varied conditions, such as high and low temperatures, would be beneficial. Lastly, since protecting the environment is becoming more important, more research should be done to find out how cement can be changed into a material that has less of an effect on the environment during loess stabilization.

Author Contributions: Conceptualization, M.A. and F.W.; Software, M.A.; Investigation, F.W. and M.-X.A.; Resources, F.W.; Writing—original draft, M.A.; Writing—review & editing, M.A. and M.-X.A.; Visualization, M.-X.A.; Supervision, X.L.; Project administration, X.L.; Funding acquisition, X.L. All authors have read and agreed to the published version of the manuscript.

Funding: This work was supported by the National Natural Science Foundation of China (grant numbers 42230712 and 41877225).

Institutional Review Board Statement: Not applicable.

Informed Consent Statement: Not applicable.

Data Availability Statement: Not applicable.

Acknowledgments: The authors acknowledge the practical support of Chang'an University.

Conflicts of Interest: The authors declare that they have no known competing financial interest or personal relationship that could have appeared to influence the work reported in this paper.

References

1. Peng, D.; Xu, Q.; Qi, X.; Fan, X.; Dong, X.; Li, S.; Ju, Y. Study on early recognition of loess landslides based on field investigation. *Int. J. Georesources Environ.* **2016**, *2*, 35–52. [CrossRef]
2. Shi, Y.-C.; Lin, X.-W.; Wang, L.-M. Earthquake damage characteristics of raw soil buildings in loess areas and disaster prevention countermeasures. *J. Nat. Disasters* **2003**, *12*, 87–92.
3. Pei, X.; Zhang, F.; Wu, W.; Liang, S. Physicochemical and index properties of loess stabilized with lime and fly ash piles. *Appl. Clay Sci.* **2015**, *114*, 77–84. [CrossRef]
4. Derbyshire, E. Geological hazards in loess terrain, with particular reference to the loess regions of China. *Earth-Sci. Rev.* **2001**, *54*, 231–260. [CrossRef]
5. Yongshuang, Z.; Yongxin, Q.U. Cements of sand loess and their cementation in north Shaanxi and west Shanxi. *Geol. Eng. J.* **2005**, *13*, 18–28.
6. Leng, Y.; Peng, J.; Wang, Q.; Meng, Z.; Huang, W. A fluidized landslide occurred in the Loess Plateau: A study on loess landslide in South Jingyang tableland. *Eng. Geol.* **2018**, *236*, 129–136. [CrossRef]
7. Jefferson, I.; Rogers, C.; Evstatiev, D.; Karastanev, D. Treatment of metastable loess soils: Lessons from Eastern Europe. In *Elsevier Geo-Engineering Book Series*; Elsevier: Amsterdam, The Netherlands, 2005; Volume 3, pp. 723–762. ISBN 1571-9960.
8. Romero, E. A microstructural insight into compacted clayey soils and their hydraulic properties. *Eng. Geol.* **2013**, *165*, 3–19. [CrossRef]
9. Qiu, H.J.; Cui, P.; Hu, S.; Liu, Q.; Wang, Y.; Gao, Y.; Deng, M. Size-frequency distribution of landslides in different landforms on the Loess Plateau of Northern Shaanxi. *Earth Sci.* **2016**, *41*, 343–350.
10. Crawford, M.M.; Bryson, L.S.; Woolery, E.W.; Wang, Z. Long-term landslide monitoring using soil-water relationships and electrical data to estimate suction stress. *Eng. Geol.* **2019**, *251*, 146–157. [CrossRef]
11. Jayasinghe, C.; Kamaladasa, N. Compressive strength characteristics of cement stabilized rammed earth walls. *Constr. Build. Mater.* **2007**, *21*, 1971–1976. [CrossRef]
12. Wang, L.; Chen, L.; Cho, D.-W.; Tsang, D.C.; Yang, J.; Hou, D.; Baek, K.; Kua, H.W.; Poon, C.-S. Novel synergy of Si-rich minerals and reactive MgO for stabilisation/solidification of contaminated sediment. *J. Hazard. Mater.* **2019**, *365*, 695–706. [CrossRef]
13. Liu, H.M.; Wang, L.M.; Gao, P. The mechanical properties of cement reinforced loess and pore microstructure characteristics. In *Applied Mechanics and Materials*; Trans Tech Publications: Stafa-Zurich, Switzerland, 2014; Volume 527, pp. 25–30.
14. James, J.; Pandian, P.K. Industrial wastes as auxiliary additives to cement/lime stabilization of soils. *Adv. Civ. Eng.* **2016**, *2016*, 1267391. [CrossRef]
15. A Rashid, A.S.; Bunawan, A.R.; Mat Said, K.N. The deep mixing method: Bearing capacity studies. *Geotech. Geol. Eng.* **2017**, *35*, 1271–1298. [CrossRef]
16. Kaniraj, S.R.; Havanagi, V.G. Compressive strength of cement stabilized fly ash-soil mixtures. *Cem. Concr. Res.* **1999**, *29*, 673–677. [CrossRef]
17. Subramanian, S.; Khan, Q.; Ku, T. Effect of sand on the stiffness characteristics of cement-stabilized clay. *Constr. Build. Mater.* **2020**, *264*, 120192. [CrossRef]
18. *EN 12390-5:2009*; Testing Hardened Concrete—Part 5: Flexural Strength of Test Specimens. iTeh Standards: Etobicoke, ON, Canada, 2009. Available online: https://standards.iteh.ai/catalog/standards/cen/275df2f9-c466-4bb1-b41c-b8dfa9fc6d89/en-12390-5-2009 (accessed on 22 March 2023).
19. *GB/T 50123-1999*; PDF in English. National Standards of the People's Republic of China: Beijing, China, 1999. Available online: https://www.chinesestandard.net/PDF.aspx/GBT50123-1999 (accessed on 22 March 2023).
20. *EN 13286-42:2003*; Unbound and Hydraulically Bound Mixtures—Part 42: Test Method for the Determination of the Indirect Tensile Strength of Hydraulically Bound Mixtures. iTeh Standards: Etobicoke, ON, Canada, 2003. Available online: https://genorma.com/en/project/show/cen:proj:10813 (accessed on 22 March 2023).
21. *ASTM D 3080*; Standard Test Method for Direct Shear Test of Soils Under Conslidated Drained Conditions—Studocu. ASTM International: West Conshohocken, PA, USA, 1998. Available online: https://www.studocu.com/en-us/document/stony-brook-university/prestressed-concrete-design/astm-d-3080-standard-test-method-for-direct-shear-test-of-soils-under-conslidated-drained-conditions/27406807 (accessed on 22 March 2023).
22. Hossain, K.M.A.; Lachemi, M.; Easa, S. Stabilized soils for construction applications incorporating natural resources of Papua New Guinea. *Resour. Conserv. Recycl.* **2007**, *51*, 711–731. [CrossRef]
23. Seco, A.; Ramírez, F.; Miqueleiz, L.; García, B. Stabilization of expansive soils for use in construction. *Appl. Clay Sci.* **2011**, *51*, 348–352. [CrossRef]
24. Kumar, A.; Walia, B.S.; Bajaj, A. Influence of fly ash, lime, and polyester fibers on compaction and strength properties of expansive soil. *J. Mater. Civ. Eng.* **2007**, *19*, 242–248. [CrossRef]
25. Kasama, K.; Zen, K.; Iwataki, K. Undrained shear strength of cement-treated soils. *Soils Found.* **2006**, *46*, 221–232. [CrossRef]
26. Consoli, N.C.; Foppa, D.; Festugato, L.; Heineck, K.S. Key parameters for strength control of artificially cemented soils. *J. Geotech. Geoenviron. Eng.* **2007**, *133*, 197–205. [CrossRef]
27. Zhang, P.; Li, Q.; Wei, H. Investigation of flexural properties of cement-stabilized macadam reinforced with polypropylene fiber. *J. Mater. Civ. Eng.* **2010**, *22*, 1282–1287. [CrossRef]

28. Consoli, N.C.; de Moraes, R.R.; Festugato, L. Parameters controlling tensile and compressive strength of fiber-reinforced cemented soil. *J. Mater. Civ. Eng.* **2013**, *25*, 1568–1573. [CrossRef]
29. *SNI 7064:2014*; Semen Portland Komposit | Perpustakaan Khazanah Analitika. Badan Standar Nasional: Jakarta, Indonesia, 2014. Available online: http://pustaka.smakbo.sch.id/index.php?p=show_detail&id=2501&keywords= (accessed on 22 March 2023).
30. Chen, T.; Gao, X. Effect of carbonation curing regime on strength and microstructure of Portland cement paste. *J. CO2 Util.* **2019**, *34*, 74–86. [CrossRef]
31. Qin, L.; Gao, X. Properties of coal gangue-Portland cement mixture with carbonation. *Fuel* **2019**, *245*, 1–12. [CrossRef]
32. Angelova, R.; Evstatiev, D. Strength grain stages of soil-cement. In Proceedings of the 6th International Congress International Association of Engineering Geology, Amsterdam, The Netherlands, 6–10 August 1990; pp. 3147–3154.